Feature Article

Photoinduced Spectral Diffusion and Diffusion-Controlled Electron Transfer Reactions in Fluorescence Intermittency of Quantum Dots

Jau Tang* (湯朝暉) and R. A. Marcus*
Noyes Laboratory of Chemical Physics, California Institute of Technology, Pasadena, CA 91125, U.S.A.

An overview is given for the experimental and theoretical development on fluorescence intermittency (blinking) in semiconductor crystalline nanoparticles. We consider a model with photoinduced spectral diffusion and diffusion-controlled electron transfer processes as the underlying mechanism for intermittency in quantum dots. Depending on the frequency response of a dielectric medium, anomalous/normal diffusion in energy space leads to power-law intermittency for single quantum dots and quasi-stretched exponential decay in ensemble-averaged fluorescence intensity. Intricate relationship between single particle and ensemble behavior is discussed. Some kinetic and energetic parameters are linked to the temporal behavior of blinking statistics and ensemble fluorescence decay.

Keywords: Quantum dots; Electron transfer; Diffusion; Nanoparticles; Single molecule spectroscopy; Fluorescence.

I. INTRODUCTION

Recent developments in nanofabrication of low-dimension materials such as quantum dots, quantum wells, quantum wires and nanotubes have generated wide interest and opened a new realm of scientific research1-3 (and references therein). For semiconductor nanocrystalline particles, or quantum dots (QDs), their unusual optical and electrical properties have found novel utilizations and have offered potential applications in biology, chemistry, physics and technology. For example, because of the size-dependent photoluminescence of QDs with a high quantumyield, QDs are being explored for biological tagging as a tracer for cancerous cells.4 Their tunability of band-gap emission with a very narrow line width and large optical strength have offered many potential applications, including new types of laser, electro-optical modulators and high density logical devices. 1-3 In addition, with chemical manipulations large-scale nano-assemblies can be made bottom-up from colloidal QDs whose sizes are easily control-

Blinking (fluorescence intermittency) phenomenon in single QDs was first reported by Brus and coworkers. ⁵ They observed that when single QDs were under continuous light illumination some went dark and became light

again stochastically. In addition, unusual power-law distribution in the histogram of the on-off (light-dark) events were noted. In this report, we present an overview of recent experimental and theoretical developments of these unusual photochemical processes involved in QDs. We discuss the roles of photoinduced spectral diffusion and electron transfer reactions involved in the mechanisms of fluorescence intermittency in QDs. We also address the intricate relationship between power-law intermittency of single QDs and the ensemble-averaged fluorescence decay which appears to follow a quasi-stretched exponential behavior. The diffusion-controlled electron transfer (DCET) model in the presence of Debye and non-Debye dielectric medium will be described.

Ever since the first observation⁴ of blinking phenomena of QDs, there has been a wealth of literature on experimental and theoretical studies of the unusual behavior. On the experimental side, several groups have made significant improvements in the understanding of these phenomena, for example, the work of Brus, ⁴⁻⁶ Bawendi, ⁸⁻¹³ Nesbitt, ¹⁴⁻¹⁷ Dahan, ¹⁸⁻²⁰ Orrit, ^{21,22} Cichos, ^{23,24} and their collaborators and of many others. ²⁵⁻²⁷ In addition to the initial observation of blinking and power law, Brus's group⁶ later identified the dark QD state as positively charged with a hole residing in the core of a QD and an electron possibly

Special Issue for the 4th Asia Photochemistry Conference, January 5~10, 2005, Taipei, Taiwan, R.O.C.

^{*} Corresponding author. E-mail: jautang@caltech.edu and ram@caltech.edu

trapped elsewhere. Nesbitt's group¹⁴ first reported $t^{-3/2-\alpha}$ power-law behavior (α a small number) for the lifetime distribution for both on and off-events. In a later study, 15 they eliminated the possibility of a static distribution of the electron/hole trapping sites. Bawendi's group linked the intermittency to photoinduced spectral diffusion, suggesting a possible role of diffusion on the power law. In a different study, they observed two emission tracks separated by 20~25 meV with QDs on a rough gold surface,11 indicating that a previously dark charged state on a quartz substrate becomes emissive. They also noted the histogram of such binary jumps also follows a t-3/2 power law. Chung and Bawendi explored the relationship between ensemble fluorescence decay12 and single QDs intermittency. Dahan and coworkers 19 demonstrated applications of QDs to biological labeling and to single photon sources. They also observed nonergodicity and addressed the relation between single particle and ensemble measurements.²¹ In Orrit's group^{21,22} intensity correlation techniques were used to study QDs. They observed a similar $t^{-3/2-\alpha}$ power law. Cichos and coworkers^{23,24} observed the correlation between the dielectric property of the tapped state and the power law. Hübner, Basche and coworkers29 and Cichos' group³⁰ independently observed a similar power-law behavior in single organic chromophores, indicating the power-law behavior is not restricted only to semiconductor nanoparticles.

On the theoretical front, understanding of the mechanisms for QD blinking phenomena and power law has been advanced by many groups, e.g., Efros and Rosen,31 Wolynes, 32 Weiss, 33 Silbery, 34 Nesbitt, 17 Bawendi, 10 Orrit, 21 Barkai, 35 Tang and Marcus, 36-38 Frantsuzov and Marcus, 39 Klafter and Szabo, 40 Osad'ko, 41 etc. Efros and Rosen 31 considered a rate equation among three states with 0, 1 and 2 electron-hole pairs to describe a random telegraph (blinking) signal. This model led to an ordinary exponential decay instead of a power law. Wang and Wolynes³² used a reaction diffusion scheme to describe Poisson statistics of intermittency in single molecules. The issues about QDs and power law were not discussed. Silbey³⁴ studied the Lévy flight model and connections to power-law behavior. Nesbitt¹⁷ used a static model with exponentially distributed distances for the tunneling rate. This model requires a very large number of surface trap sites over a wide distance range to accommodate 7 to 8 decades for the dynamic range of blinking statistics. Bawendi 10 described a discrete-time random walk model for a dark trap state in resonance with the excited states of QDs. They suggested this intrinsic hopping time depends on temperature, and light intensity at cryogenic temperatures. Orri²¹ presented a model that relates the exponent of the power law to potential of the electron in the QD, in the matrix and in the traps. It remains to be explored for this model to explain why most of the observed exponents in QDs are close to -3/2. Klafter and Szabo⁴⁰ explored two-state single-molecule trajectories arising from a multi-substrate kinetics.

Weiss³³ described a stochastic two-state model and obtained some relations between the lifetime distribution function for intermittency and the ensemble intensity. Such a model was applied by Margolin and Barkai³⁵ to various cases where intermittency can be described by a power law or an exponential decay. These relations can also be derived using our DCET (diffusion-controlled electron transfer) model, which provides a molecular basis and physical insight into the kinetic parameters and into the stochastic nature of energy fluctuations. In two recent studies^{39,41} Auger-assisted electron transfer for deep traps was invoked. Because intermittency was also observed in organic chromophores, it remains to be explored if the electronic coupling in these systems also involves such Auger-assisted processes.

To improve our understanding of the underlying mechanism for fluorescence intermittency and the power law, we recently proposed a diffusion-controlled electron transfer (DCET) mechanism^{36,37} to elucidate short-time behavior of single QDs and quasi-stretched exponential decay³⁸ of fluorescence intensity decay $\langle I(t)\rangle$ of a QD ensemble. The diffusion-reaction model was first considered by Zusman⁴² for electron transfer and has since then been extensively used by many others. ⁴³⁻⁴⁷ In this overview, we focus first on light-induced spectral diffusion, analyze next the intermittency for single QDs, and finally discuss the ensemble behavior of $\langle I(t)\rangle$ over the entire time span and investigate its relationship to lifetime distribution P(t) for both light and dark-events in single QDs.

II. DIFFUSION-CONTROLLED ELECTRON TRANSFER MODEL

In this main section about the theoretical model, our presentation is divided into five topics, (A) single particle vs. ensemble, (B) electronic states relevant to intermittency, (C) photoinduced spectral diffusion, (D) intermit-

tency of single QDs and power law, and (E) ensembleaveraged fluorescence intensity.

A. Single particle vs. ensemble

Before addressing the issues about fluorescence intermittency in single QDs and the ensemble-averaged fluorescence, we would like to consider whether ergodicity applies in QDs, i.e., whether the time-average of singleparticle behavior is equivalent to ensemble-averaged behavior. There are subtle differences between single-QD behavior and ensemble behavior. In intermittency measurements, one observes the fluorescence intensity of a single OD under continuous illumination. A histogram illustrated in Fig. 1 is recorded for an individual single QD that undergoes stochastic exchanges between a light state |1> and a dark state |2>. In such a study a QD is distinguishable from the others, and its histogram shows binary jumps between two levels, "on" or "off". The charged state |2> appears dark due to quenching by a fast radiationless Auger process. From the histogram one can determine the duration of "on" or "off" periods and display the probability distribution $P_{on}(t)$ or $P_{off}(t)$ of the duration time for the "on" or "off" events. On the other hand, in ensemble measurements, the fluorescence intensity is recorded from large numbers of QDs which are indistinguishable. The detector can not tell which QD emits a photon, and a priori knowledge is lacking about the history of an individual QD. En-

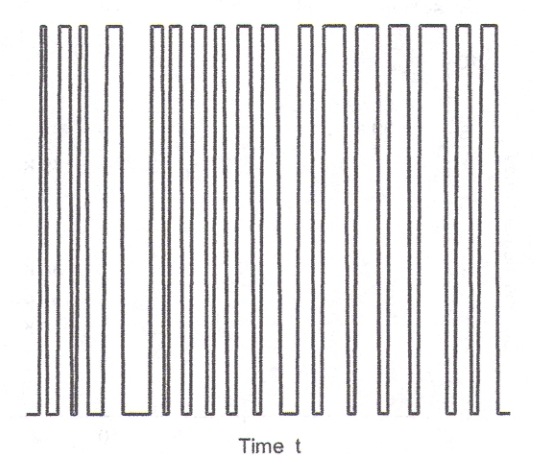


Fig. 1. A schematic histogram of fluorescence intermittency showing stochastic binary jumps between two intensity levels. Blinking statistics P(t) is defined as the lifetime distribution for the duration periods for the "on" or "off" events.

semble-averaged fluorescence decay actually represents the sum of the histograms from all QDs. Therefore, to describe $\langle I(t)\rangle$ for an ensemble one needs to use coupled rate equations including both forward and reverse reactions, whereas to describe either $P_{on}(t)$ or $P_{off}(t)$ of a single QD only a forward or reverse rate equation needs to be used. Therefore, the nonergodic nature of QDs needs to be understood from the context of the fact that in P(t) of single-particle studies a QD is distinguishable whereas in ensemble measurements of $\langle I(t) \rangle$ QDs are indistinguishable.

B. Electronic states relevant to intermittency

Semiconductor crystalline nanoparticles, or quantum dots as they are often called, used in intermittency studies are made of CdSe, CdTe, InS, and other compositions. The usual size is about 1 to 4 nm in radius. As semiconductors in bulk, the band gap of QDs is of the order of a few meV, but tunable by sizes. In addition, due to quantum size effects QDs contain discrete electronic structure instead of the continuous conduction and valence bands as in bulk materials. Several relevant electronic states, their relaxation pathways and rate constants, play a key role in intermittency are illustrated in Fig. 2.

C. Photoinduced spectral diffusion

According to the observation by Empedocles et al.,9 the spectral line width of band edge emission increases with time and light intensity. To describe such a spectral diffusion process, we consider in Fig. 3 two parabolic potentials with q as the reaction coordinate. The q_0 there is the horizontal displacement between the potential well $U_1(q)$ = $\kappa q^2/2$ for the light state |1> and $U_0(q) = \kappa (q + q_0)^2/2 - E_q$ for the ground state |0>, and E_g is the free energy gap.

The rate equation for population f(q, t) in state $|1\rangle$ is the well-known Smoluchowski diffusion equation

$$\frac{\partial}{\partial t} f(q,t) = \frac{\Delta_1^2}{\tau_1} \left(\frac{\partial^2}{\partial q^2} f(q,t) + \frac{1}{k\Delta_1^2} \frac{\partial}{\partial q} \left(f(q,t) \frac{\partial}{\partial q} U_1(q) \right) \right), \tag{1}$$

where the diffusion constant $D_1 = \Delta_1^2/\tau_I$, and $\kappa \Delta_1^2 \sim k_B T$ in the high temperature limit. Its Green function G(q,q';t), the probability of finding a QD at point q' at time t that was initially at q, is given by 36

$$G(q, q'; t) = \frac{1}{\sqrt{2\pi\Delta_1^2 \left(1 - \exp(-2t/\tau_1)\right)}} \times \exp\left[-\frac{\left(q - q'\exp(-t/\tau_1)\right)^2}{2\Delta_1^2 \left(1 - \exp(-2t/\tau_1)\right)}\right].$$
(2)

Based on the Franck-Condon principle, the spectral emission energy, $\Delta U(q) = U_1(q) - U_0(q)$, changes in time and results in spectral diffusion. The second moment of the emission spectrum is given by

$$\sigma^{2}(t) = \left\langle \left(\Delta U(q) - \left\langle \Delta U(q) \right\rangle \right)^{2} \right\rangle$$

$$= \int_{-\infty}^{\infty} dq (\kappa \, qq_{0})^{2} \, G(q, q; t)$$

$$= 2\kappa \Lambda \Delta_{1}^{2} \left[1 - \exp(-t/\tau_{1}) \right], \tag{3}$$

where $\Lambda = \kappa q_0^2/2$, is the "excitation reorganization energy" and 2Λ the Stokes shift.

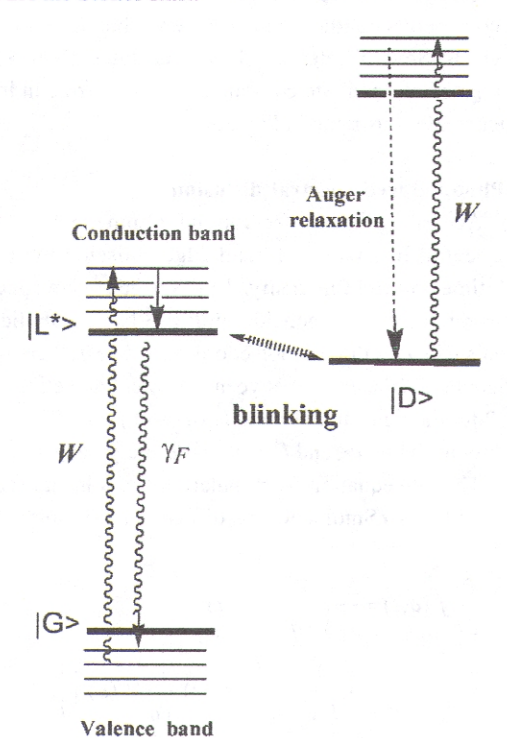


Fig. 2. A schematic energy diagram for a QD, showing conduction band above the lowest excited state |L*> and the valence bands below |G>, and other states relevant to blinking. Fast Auger relaxation processes cause the positively charged |2> to appear dark.

Spectral linewidth data of CdSe QDs by Empedocles et al. 9 were converted to spectral second moments and plotted in Fig. 4, with a universal variable "energy density" (time t times light intensity). The data were fitted to Eq. (3) with an inverse dependence of τ_1 on light intensity, based on the light-induced diffusion assumption.

D. Intermittency of single QDs and power law

According to the first-passage time theory, ⁴⁸ an N-dimensional diffusion with an (N-1)-dimensional absorbing surface boundary results in a $t^{(N+2)/2}$ power law for the surviving probability. Initial observation of $t^{-3/2}$ power-law

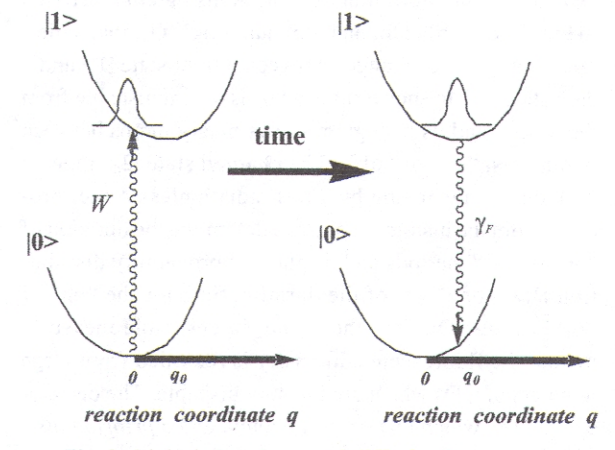


Fig. 3. Light-induced spectral diffusion between the ground state and the photoexcited state.

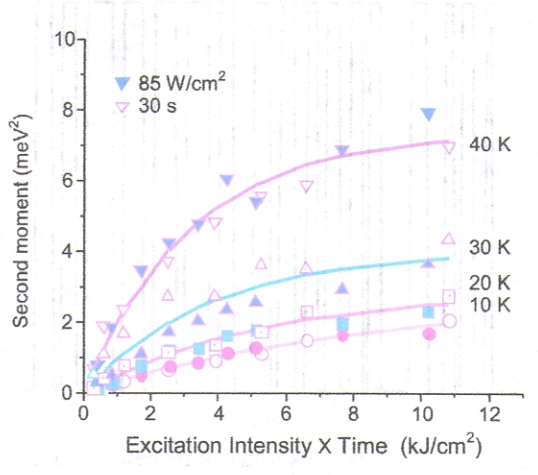


Fig. 4. The spectral second moment vs. energy density (light intensity times evolution time t). The experimental data of CdSe (taken from Empedocles and Bawendi⁹) were fitted by Eq. (3) to extract diffusion correlation time constant.³⁶

intermittency in QDs prompted the hypothesis of 1-D diffusion of the electron/hole among discrete localized surface traps. However, such a discrete hopping mechanism is faulty. To account for 7 to 8 decades for the observed P(t), ¹⁷ the number of the localized traps has to exceed 500, as illustrated in Fig. 5; in addition, these localized traps have to be aligned in a 1-D fashion for this 1-D mechanism to work. A QD of 2 to 4 nm in radius would not contain so many surface traps that can line up in an 1-D array. Therefore, the 1-D diffusion is likely to operate in a configuration space, such as in energy space as suggested by Bawendi's group⁹ from photoinduced spectral diffusion measurements.

To be more general and to accommodate a power law with an exponent that could differ from the ideal -3/2, we considered a non-Markovian anomalous diffusion in the diffusion-controlled electron transfer model between a dark charged state and a light neutral state, and the ordinary Markovian diffusion is thus treated as a special case.³⁷

In treating anomalous diffusion in electron/energy transfer reactions, there are two often used approaches: POP (partial ordering prescription) and COP (chronological ordering prescription)^{49,50} (with details and references given). One can use a simplified three-state model of Fig. 6 to represent the more elaborate electronic states depicted in Fig. 2. In the POP scheme for ET, such a three-state system, the rate equation contains a time-dependent diffusion constant as³⁸

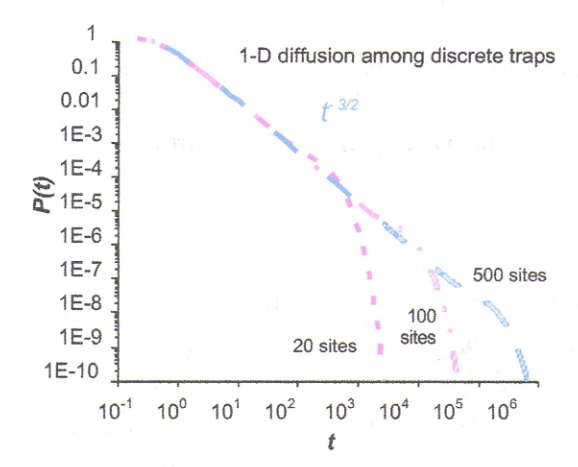


Fig. 5. A simplified three-state model with binary jumps (blinking) between a "light" state |1> and a "dark state" |2>, |1> is accessed by photoexcitation from the ground state |0>.

$$\frac{\partial}{\partial t} \rho_{1}(Q,t) = D(t) \frac{\partial}{\partial Q} \left(\frac{\partial}{\partial Q} + \frac{1}{k_{B}T} \frac{\partial}{\partial Q} U_{1}(Q) \right) \rho_{1}(Q,t)
- \frac{2\pi |V_{ex}|^{2}}{\hbar} \delta \left(U_{12}(Q) \right) \left(\rho_{1}(Q,t) - \rho_{2}(Q,t) \right)
- \gamma_{0} \rho_{1}(Q,t) + W \rho_{0}(Q,t)
\frac{\partial}{\partial t} \rho_{2}(Q,t) = D_{2}(t) \frac{\partial}{\partial Q} \left(\frac{\partial}{\partial Q} + \frac{1}{k_{B}T} \frac{\partial}{\partial Q} U_{2}(Q) \right) \rho_{2}(Q,t)
- \frac{2\pi |V_{ex}|^{2}}{\hbar} \delta \left(U_{12}(Q) \right) \left(\rho_{2}(Q,t) - \rho_{1}(Q,t) \right)
\frac{\partial}{\partial t} \rho_{0}(Q,t) = \gamma_{0} \rho_{1}(Q,t) - W \rho_{0}(Q,t).$$
(4a)

After the initial transient, a quasi-equilibrium is established between $|0\rangle$ and $|1\rangle$, and Eq. (4a) can be simplified to a two-state equation as³⁸

$$\frac{\partial}{\partial t} \rho_{1}(Q, t) = D_{1}(t) \frac{\partial}{\partial Q} \left(\frac{\partial}{\partial Q} + \frac{1}{k_{B}T} \frac{\partial}{\partial Q} U_{1}(Q) \right) \rho_{1}(Q, t) \\
- \frac{2\pi |V_{1}|^{2}}{\hbar} \delta \left(U_{12}(Q) \right) \left(\rho_{1}(Q, t) - \rho_{2}(Q, t) \right) \right) \\
\frac{\partial}{\partial t} \rho_{2}(Q, t) = D_{2}(t) \frac{\partial}{\partial Q} \left(\frac{\partial}{\partial Q} + \frac{1}{k_{B}T} \frac{\partial}{\partial Q} U_{2}(Q) \right) \rho_{2}(Q, t) \\
- \frac{2\pi |V_{2}|^{2}}{\hbar} \delta \left(U_{12}(Q) \right) \left(\rho_{2}(Q, t) - \rho_{1}(Q, t) \right), (4b)$$

Light State Dark State

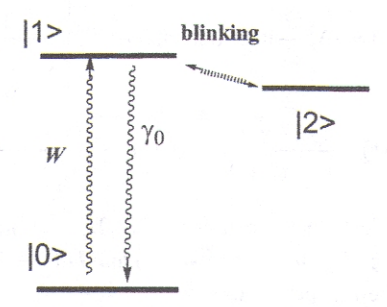


Fig. 6. Blinking statistics *P*(*t*) for 1-D diffusion among N discrete trap sites with an absorbing sink. The number of decades for the power-law behavior depends on N. In order to have *P*(*t*) cover eight decades of dynamic range, far greater than 500 discrete in-line trap sites are required. Because such a large number of trap sites is unrealistic for a small QD, this trap model has been ruled out.

where $D_1(t) \equiv \varsigma_1 D(t)$, $|V_k|^2 \equiv \varsigma_k |V_{ex}|^2$, $\varsigma_1 \equiv W/(W + \gamma_0) \sim W/\gamma_0$, $\varsigma_2 \equiv 1$ and V_{ex} the electronic coupling. Because ς_1 increases with light intensity, so does the effective diffusion coefficient D_1 .

As discussed earlier in Sec. II.A, to describe intermittency for single QDs, one should use a decoupled rate equation. For the "on" events the forward ET equation is given by³⁷

$$\frac{\partial}{\partial t} \rho_{1}(Q, t) = D_{1}(t) \frac{\partial}{\partial Q} \left(\frac{\partial}{\partial Q} + \frac{1}{k_{B}T} \frac{\partial}{\partial Q} U_{1}(Q) \right) \rho_{1}(Q, t) - \frac{2\pi |V_{1}|^{2}}{\hbar} \delta \left(U_{12}(Q) \right) \rho_{1}(Q, t), \tag{5}$$

and for the "off" events the reverse ET rate equation is given by

$$\frac{\partial}{\partial t} \rho_2(Q, t) = D_2(t) \frac{\partial}{\partial Q} \left(\frac{\partial}{\partial Q} + \frac{1}{k_B T} \frac{\partial}{\partial Q} U_2(Q) \right) \rho_2(Q, t) - \frac{2\pi |V_2|^2}{\hbar} \delta(U_{12}(Q)) \rho_2(Q, t).$$
(6)

Here we consider harmonic potentials $U_{12}(Q) = U_1(Q) - U_2(Q)$, $U_1(Q) = \kappa(Q - Q_{0,1})^2/2$, $U_2(Q) = \kappa(Q - Q_{0,2})^2/2 + \Delta G^0$, κ the force constant and $\kappa \Delta_k^2 = k_B T$, ΔG^0 the free energy gap, $\lambda = \kappa(Q_{0,1} - Q_{0,2})^2/2$ the reorganization energy and V_k the electronic coupling. The time-dependent diffusion coefficient $D_2(t)$ is related to dielectric function, $\varepsilon_k(t)$ by 37,49

$$D_{k}(t) = -\Delta_{k}^{2} \frac{d}{dt} \ln \Theta_{k}(t), \ \Theta_{k}(t) \equiv L^{-1} \left(\frac{1}{s + \frac{1}{\tau_{L,k}(s)}} \right)$$

$$\overline{\tau_{L,k}(s)} = \frac{\varepsilon_{\infty}}{\varepsilon_{0}} \frac{1 - \overline{\chi_{k}(s)}}{s \overline{\chi_{k}(s)}}, \ \overline{\chi_{k}(s)} = \frac{\overline{\varepsilon_{k}(s) - \varepsilon_{\infty}}}{\varepsilon_{0} - \varepsilon_{\infty}}.$$
(7)

For a Debye dielectric medium $\overline{\chi}(s) = 1/(1+s\,\tau_D)$, $\overline{\tau}_{L,k}(s) = \tau_{L,k} \equiv \tau_{D,k}\,\varepsilon_{\infty}/\varepsilon_0$, $\Theta_k(t) = \exp(-t/\tau_{L,k})$ and $D_k(t) = \Delta_k^2/\tau_{L,k}$ becomes time-independent.

A histogram, illustrated in Fig. 1, consists of many stochastic jumps between binary levels, representing "light" and "dark" levels. Each blinking event for a QD starts with the reaction coordinate Q at the energy-level crossing, i.e., $\rho_k(Q, 0) = \delta(Q - Q_c)$, as shown in Fig. 7. The surviving probability $P_{on}(t)$ for the "on"-events of a single QD, or $P_{off}(t)$ for the "off"-events, is defined as the waiting time distri-

bution function for a QD at Q_c and is turned into the "dark state" (or "light" state) between t and t + dt per unit dt. The Green function for sink-free diffusion in a harmonic potential $\kappa q^2/2$ is given by 37,49

$$G_{k}(q,q';t) = \frac{1}{\sqrt{2\pi\Delta_{k}^{2}\left(1-\Theta_{k}^{2}(t)\right)}} \exp\left[-\frac{\left(q-q'\Theta_{k}(t)\right)^{2}}{2\Delta_{k}^{2}\left(1-\Theta_{k}^{2}(t)\right)}\right], (8)$$

Eqs. (5) and (6) can be solved by the Green function method and Laplace transform. We obtained the Laplace transform of P(t) as

$$\overline{P_k}(s) = -\int_0^\infty dt \ e^{-st} \frac{d}{dt} \left(\int_{-\infty}^\infty dQ \ \rho_k(Q, t) \right) = \frac{A_k \overline{G}_k(Q_c, Q_c; s)}{1 + A_k \overline{G}_k(Q_c, Q_c; s)}$$

$$A_k = \frac{2\pi}{\hbar} |V_k|^2 \left| \partial \left(U_1(Q) - U_2(Q) \right) \middle/ \partial Q \right|_{Q = Q_c}. \tag{9}$$

Defining $\overline{g}_k(s) = A_k \overline{G}_k(Q_c, Q_c; s)$, $\overline{P}_k(s)$ of a single QD can be established via $\overline{g}_k(s)$ obtained previously^{36,37}

$$\overline{P}_k(s) = \frac{\overline{g}_k(s)}{1 + \overline{g}_k(s)}, \quad \overline{g}_k(s) = \frac{\overline{P}_k(s)}{1 - \overline{P}_k(s)}.$$
 (10)

For a Cole-Davison dielectric medium⁵¹ $\overline{\chi}(s) = 1/(1+s \tau_D)^{\beta_{CD}}$, one obtains an asymptote $\overline{g}_k(s) \approx ((s+\Gamma_k)t_{c,k})^{\beta_{CD}/2-1}$ if $s > \Gamma_k$. Inverse Laplace transform of Eq. (10) yields

$$\overline{P}_k(s) \approx \frac{1}{1 + \left(\left(s + \Gamma_k \right) t_{c,k} \right)^{1 - \beta_{CD}/2}}.$$
(11)

By inverse Laplace transform of Eq. (11), one has³⁷

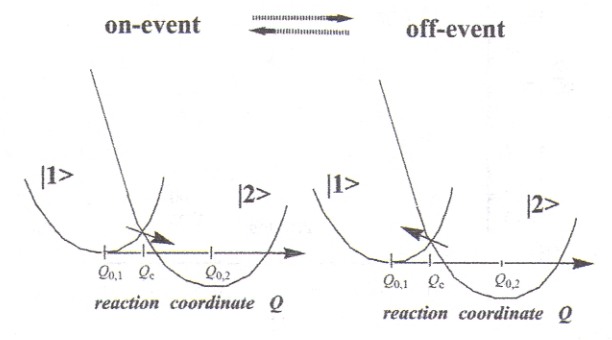


Fig. 7. Intermittency as controlled by 1-D diffusion in energy space via a sink at the energy-level crossing of two parabolic potential wells of a light |L> state and a dark |D> state.

$$\begin{split} P_k(t) &\sim \frac{d}{dt} \left[E_{-1+\beta_{CD}/2} \left(-(t/t_{c,k})^{-1+\beta_{CD}/2} \right) \right] \exp(-\Gamma_k t) \\ &\qquad \qquad \text{if} \quad t \leq 1/\Gamma_k < \tau_{L,k} \\ P_k(t) &\sim \left(t/t_{c,k} \right)^{-\beta_{CD}/2} \left/ \Gamma \left(1 - \beta_{CD}/2 \right) t_{c,k} , \quad \text{if} \quad t < t_{c,k} \\ P_k(t) &\sim \left(t/t_{c,k} \right)^{-2+\beta_{CD}/2} \exp(-\Gamma_k t) \middle/ \left| \Gamma \left(\beta_{CD}/2 - 1 \right) t_{c,k} \right| \\ &\qquad \qquad \text{if} \quad t_{c,k} < t \leq 1/\Gamma_k < \tau_{L,k} \end{split} \tag{12}$$

where

$$\left(t_{c,k}/\tau_{D,k}\right)^{\beta_{CD}}/t_{c,k}^{2} \equiv \pi \left|V_{k}\right|^{4} \tau_{L,k} \Gamma(\beta_{CD}+1)/2\lambda \ k_{B} T \hbar^{2} \tau_{D,k}
\left(\Gamma_{k} \tau_{D,k}\right)^{\beta_{CD}} \equiv E_{A,k} \tau_{D,k}/2k_{B} T \tau_{L,k} \Gamma(\beta_{CD}+1),$$
(13)

and $E_a(z) = \sum_{n=0}^{\infty} z^n / \Gamma(na+1)$, is the Mittag-Leffler function. 52 As illustrated in Fig. 8, $P_k(t)$ of Eq. (12) follows two power laws with an exponent of $-\beta_{CD}/2$ at $t < t_{c,k}$ and another exponent of $-2 + \beta_{CD}/2$ at $t > t_{c,k}$.

For the normal diffusion case in a Debye medium with $\beta_{CD} = 1$, Eq. (12) can be simplified to³⁶

$$P_{k}(t) = \frac{1}{\sqrt{\pi t_{c,k}t}} \left[1 - \sqrt{\pi t/t_{c,k}} \exp(t/t_{c,k}) \right]$$

$$\times \operatorname{erfc}\left(\sqrt{t/t_{c,k}}\right) \exp(-\Gamma_{k}t), \tag{14}$$

and

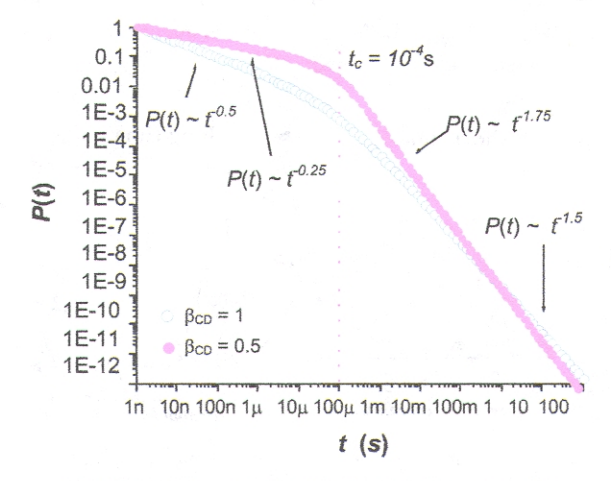


Fig. 8. Blinking statistics P(t) for DCET model with normal diffusion ($\beta_{CD} = 1$) and anomalous diffusion ($\beta_{CD} \neq 1$). The exponent for the power law depends on β_{CD} of the dielectric medium. At a much shorter time than t_c (set arbitrarily at 10^{-4} s), P(t) follows a different power law.

$$P_{k}(t) \sim \frac{1}{\sqrt{\pi t_{c,k}}} t^{-\frac{1}{2}} \qquad \text{if} \quad t << t_{c,k}$$

$$P_{k}(t) \sim \frac{\sqrt{t_{c,k}}}{2\sqrt{\pi}} t^{-\frac{3}{2}} \exp(-\Gamma_{k}t) \quad \text{if} \quad t_{c,k} << t << \tau_{L,k} \ (15)$$

where

$$\Gamma_{k}\tau_{k} \equiv \frac{E_{A,k}}{2k_{B}T}, \quad E_{A,1} \equiv \frac{\left(\lambda + \Delta G^{0}\right)^{2}}{4\lambda}, \quad E_{A,2} \equiv \frac{\left(\lambda - \Delta G^{0}\right)^{2}}{4\lambda}$$

$$E_{A,1} - E_{A,2} = \Delta G^{0}, \quad 2\Gamma_{1}\tau_{1} - 2\Gamma_{2}\tau_{2} = \frac{\Delta G^{0}}{k_{B}T}. \tag{16}$$

From Eq. (15) for a Debye dielectric medium, two exponents exist for the power law, i.e., -1/2 at $t < t_{c,k}$ and -3/2 at t $> t_{c,k}$. As an example of the applications of the DCET model, experimental data of CdTe QDs by Shimizu et al.¹⁰ are illustrated in Fig. 9, showing good agreement with Eq. (15). Because diffusion is light-induced, as light intensity increases τ_1 is shortened, and according to Eq. (16) Γ_1 increases and the exponential bending tail for the "on" events appears. For the "off" events, the light-dependence of diffusion in the dark state is diminished by a fast Auger relaxation, τ_2 is substantially longer than τ_1 . The exponential bending for the "off" events is expected to occur much later

In the long-time limit $(t >> \tau_{L,k}) \overline{g_k}(s) \approx \gamma_k / s + f_k$, Eq.

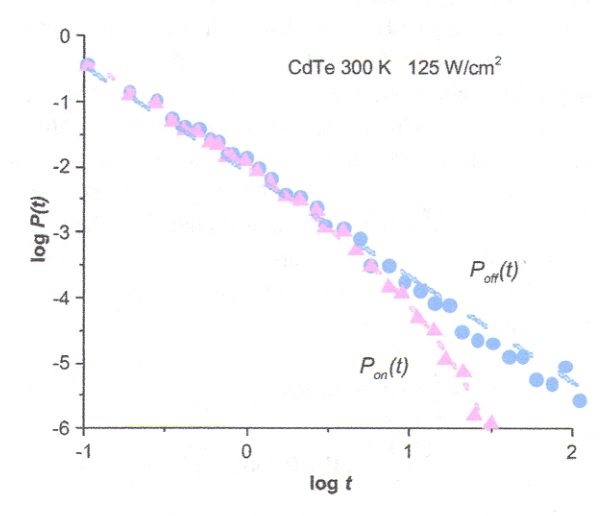


Fig. 9. The log-lot plot of t P(t) vs, time t for data of both "off" and "on" events of CdTe QDs at 300 K and 125 W/cm2 (taken from the Shimizu et al. 10). The data were fitted to Eq. (15).

(10) yields³⁷

$$P_{k}(t) \approx \frac{\gamma_{k,eff}}{1 + f_{k}} \exp(-\gamma_{k,eff}t), \ \gamma_{k,eff} \equiv \frac{\gamma_{k}}{1 + f_{k}},$$

$$\gamma_{k} \equiv \frac{A_{k}}{\sqrt{2\pi\Delta_{k}^{2}}} \exp(-E_{A,k}/k_{B}T)$$

$$= \frac{2\pi}{\hbar} \frac{|V_{k}|^{2}}{\sqrt{4\pi\lambda_{k}T}} \exp(-E_{A,k}/k_{B}T)$$
(17)

where

$$f_{k} \equiv \int_{0}^{\infty} dt \left[A_{k} \exp\left(-2\Gamma_{k} \tau_{L,k} \tanh(t/2\tau_{L,k})\right) \right] / \sqrt{2\pi \Delta_{k}^{2} \left(1 - \exp(-2t/\tau_{L,k})\right)} - \gamma_{k} \right].$$
 (18)

Details about evaluation of f_k have been provided by Rips and Jortner.⁵³ Eq. (17) indicates that $P_k(t)$ for both "on" and "off" events would decay exponentially.

E. Ensemble-averaged fluorescence intensity

As discussed earlier, to treat ensemble-averaged fluorescence intensity one has to use the coupled rate equation with both forward and reverse electron transfer. In Eq. (4) a POP approach was used. In the above single-QD intermittency study only the short time power-law behavior was of major interest. To calculate longer time behavior for a single QD or the ensemble fluorescence intensity over the entire time span, one needs to solve Eq. (4) in Laplace transform. Because Eq. (4) of POP scheme involves a product in the time domain of $D_k(t)$ and a diffusion operator on timedependent population $\rho_k(t)$, it becomes a convoluted integral in the Laplace transform domain and much more difficult to handle numerically. Therefore, in the treatment of this section we chose the other COP approach which involves convolution in the time domain but a simpler product form in the Lapalce transform domain.

The coupled rate equation for electron transfer in the COP scheme is given by

$$\frac{\partial}{\partial t} \rho_{1}(Q, t) = \int_{0}^{t} d\tau L_{1}(t - \tau) \rho_{1}(Q, \tau)$$

$$-\frac{2\pi |V_{1}|^{2}}{\hbar} \delta(U_{12}(Q)) (\rho_{1}(Q, t) - \rho_{2}(Q, t))$$

$$\frac{\partial}{\partial t} \rho_{2}(Q, t) = \int_{0}^{t} d\tau L_{2}(t - \tau) \rho_{2}(Q, \tau)$$

$$-\frac{2\pi |V_{2}|^{2}}{\hbar} \delta(U_{12}(Q)) (\rho_{2}(Q, t) - \rho_{1}(Q, t)) \quad (19)$$

where
$$L_k(\tau) \equiv \Delta_k^2 \, \varphi_k(\tau) \frac{\partial}{\partial Q} \left(\frac{\partial}{\partial Q} + \frac{\partial}{\partial Q} (U_k(Q) / k_B T) \right)$$
, and

 $\overline{\varphi}_k(s) = (s\tau_{D,k} + 1)^{1-\beta_{VD}}/\tau_{L,k}$. Eq. (19) becomes Markovian if $\beta_{CD} = 1$ where $\varphi_k(t) = \delta(t)/\tau_{L,k}$. Most of the expressions derived earlier in this study by POP approach can also be obtained by COP. Both approaches yield similar asymptotic results at very short or long times; differences in the midtime regime are assumed to be small. Defining $\overline{G}_k(Q,Q';s)$, the Green function in the Laplace transform domain, that satisfies $s\overline{G}_k(Q,Q';s) - \overline{L}_k(s)\overline{G}_k(Q,Q';s) = \delta(Q-Q')$, one obtains from Eq. (19)

$$\langle \overline{\rho}_{1}(s) \rangle \equiv \int_{-\infty}^{\infty} dQ \overline{\rho}_{1}(Q, s) = \frac{1}{s} \int_{-\infty}^{\infty} dQ \rho_{1}(Q, 0)$$

$$= \int_{-\infty}^{\infty} dQ A_{1} \overline{G}_{1}(Q_{c}, Q; s) \rho_{1}(Q, 0) - \int_{-\infty}^{\infty} dQ A_{2} \overline{G}_{2}(Q_{c}, Q; s) \rho_{2}(Q, 0)$$

$$= \frac{1}{s} \int_{-\infty}^{\infty} dQ A_{1} \overline{G}_{1}(Q_{c}, Q; s) \rho_{1}(Q, 0) - \int_{-\infty}^{\infty} dQ A_{2} \overline{G}_{2}(Q_{c}, Q; s) \rho_{2}(Q, 0)$$

$$= \frac{1}{s} \int_{-\infty}^{\infty} dQ \overline{\rho}_{1}(Q, Q; s) \rho_{1}(Q, 0) - \int_{-\infty}^{\infty} dQ A_{2} \overline{G}_{2}(Q_{c}, Q; s) \rho_{2}(Q, 0)$$

$$= \frac{1}{s} \int_{-\infty}^{\infty} dQ A_{1} \overline{G}_{1}(Q_{c}, Q; s) \rho_{1}(Q, 0) - \int_{-\infty}^{\infty} dQ A_{2} \overline{G}_{2}(Q_{c}, Q; s) \rho_{2}(Q, 0)$$

$$= \frac{1}{s} \int_{-\infty}^{\infty} dQ A_{1} \overline{G}_{1}(Q_{c}, Q; s) \rho_{1}(Q, 0) - \int_{-\infty}^{\infty} dQ A_{2} \overline{G}_{2}(Q_{c}, Q; s) \rho_{2}(Q, 0)$$

$$= \frac{1}{s} \int_{-\infty}^{\infty} dQ A_{1} \overline{G}_{1}(Q_{c}, Q; s) \rho_{1}(Q, 0) - \int_{-\infty}^{\infty} dQ A_{2} \overline{G}_{2}(Q_{c}, Q; s) \rho_{2}(Q, 0)$$

$$= \frac{1}{s} \int_{-\infty}^{\infty} dQ A_{1} \overline{G}_{1}(Q_{c}, Q; s) \rho_{1}(Q, 0) - \int_{-\infty}^{\infty} dQ A_{2} \overline{G}_{2}(Q_{c}, Q; s) \rho_{2}(Q, 0)$$

$$= \frac{1}{s} \int_{-\infty}^{\infty} dQ A_{1} \overline{G}_{1}(Q; Q; q; s) \rho_{1}(Q; q; s) \rho_{2}(Q; q; s) \rho_{2}(Q; q; s) \rho_{2}(Q; q; s)$$

If an ensemble of QDs is initially at Q_c , the energy level crossing, with $\rho_1(Q,0) = C \delta(Q - Q_c)$ and $\rho_2(Q,0) = (1 - C) \delta(Q - Q_c)$, Eq. (20) yields

$$\left\langle \overline{\rho}_{1}(s) \right\rangle_{Xing} = \frac{C}{s} - \frac{1}{s} \frac{C\overline{g}_{1}(s) - (1 - C)\overline{g}_{2}(s)}{1 + \overline{g}_{1}(s) + \overline{g}_{2}(s)}.$$
 (21)

If a QD ensemble is initially in |1> as illustrated in Fig. 10 with a Boltzmann distribution $\rho_1(Q,0) = (1/\sqrt{2\pi k_B T/\kappa})$ exp $(-\kappa(Q-Q_{0,1})^2/2k_BT)$, the normalized intensity $\langle \tilde{I}(s) \rangle$ can be derived from Eq. (20) and³⁸

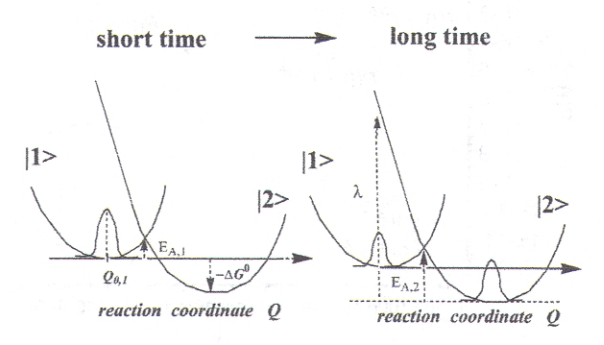


Fig. 10. Time evolution of an initial population profile in $|1\rangle$ centered at $Q_{0,1}$. At longer times a steady-state distribution is established between $|1\rangle$ and $|2\rangle$. The relation of forward/reverse ET activation energy $(E_{A,1}/E_{A,2})$, reorganization energy (λ) and free energy gap (ΔG^0) to two parabolas is illustrated.

$$\langle \overline{I}(s) \rangle = \langle \overline{\rho}_1(s) \rangle = \frac{1}{s} \left[1 - \frac{\gamma_1}{s \left(1 + \overline{g}_1(s) + \overline{g}_2(s) \right)} \right], \quad (22)$$

where γ_1 and γ_2 are the nonadiabatic forward and reverse reaction rates. Defining the relaxation function $\langle \overline{R}(s) \rangle$ as $\langle \overline{R}(s) \rangle (1 - I_{eq}) \equiv \langle \overline{I}(s) \rangle - I_{eq}/s$, from Eq. (22), one has

$$\left\langle \overline{R}(s) \right\rangle = \frac{1}{s} \left[1 - \frac{\gamma_1 + \gamma_2}{s \left(1 + \overline{g}_1(s) + \overline{g}_2(s) \right)} \right] \tag{23}$$

The steady-state intensity is given by³⁸

$$I_{eq} = \frac{1}{1 + \varsigma_1 \exp(-\Delta G^0 / k_B T)}.$$
 (24)

Using the relationship between $\overline{P}_k(s)$ of single QDs and $g_k(s)$ one can express Eq. (21) as

$$\left\langle \overline{\rho_1}(s) \right\rangle_{Xing} = \frac{1 - \overline{P_1}(s)}{s} \cdot \frac{C + (1 - C)\overline{P_2}(s)}{1 - \overline{P_1}(s)\overline{P_2}(s)}. \tag{25}$$

One can also express Eq. (22) as³⁸

$$\langle \overline{I}(s) \rangle = \frac{1}{s} \left[1 - \frac{\gamma_1 \left(1 - \overline{P}_1(s) \right) \left(1 - \overline{P}_2(s) \right)}{s \left(1 - \overline{P}_1(s) \overline{P}_2(s) \right)} \right]$$
(26)

and Eq. (23) as

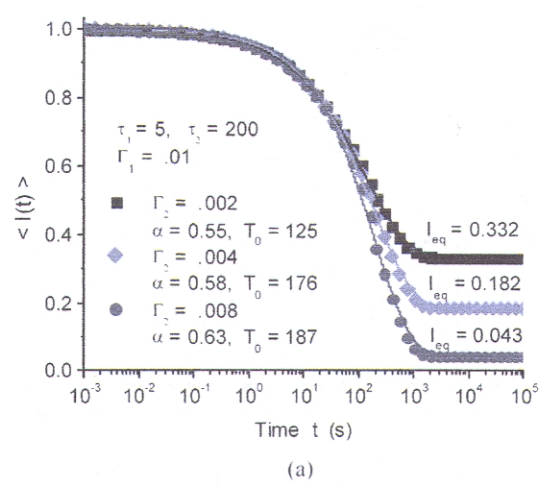
$$\left\langle \overline{R}(s) \right\rangle = \frac{1}{s} \left[1 - \frac{\gamma_1 + \gamma_2}{s} \frac{\left(1 - \overline{P}_1(s) \right) \left(1 - \overline{P}_2(s) \right)}{1 - \overline{P}_1(s) \overline{P}_2(s)} \right]. \tag{27}$$

Eqs. (25-27) represent relationships between ensembleaveraged behavior and blinking statistics $\overline{P}_k(s)$ of single QDs. The Stokes shift was not included in deriving Eqs. (22-27) if the initial population is not centered at $Q_{0,1}$. More details and the roles of band-edge electronic structures will be discussed elsewhere.55

Eqs. (25-27) have been derived previously by Weiss and his coworkers, 33 and were applied by others, including Dahan, 20 Orrit21,22 and Barkai35 to characterize asymptotic behavior of QDs. Eq. (25) only applies when an initial population is at the energy level crossing, and was used previously by Bardou et al.53 for laser cooling, and was recently applied by Chung and Bawendi¹² to ensemble studies. These equations were previously expressed in terms of $\overline{P}_k(s)$ and $\langle \tau_k \rangle$. Here, we show $\langle \tau_k \rangle^{-1} = \gamma_k$, and is simply the non-adiabatic electron transfer rate. More importantly, via

 $\overline{g}_{\ell}(s)$ Eqs. (21-23) provide formulas calculable for the entire time span (for anomalous/normal diffusion model), and link $\langle I(t) \rangle$ and $P_k(t)$ to measurable molecular-based quanti-

Some calculated curves based on Eq. (22) with a Debye medium are illustrated in Fig. 11, showing a fit to a stretched exponential $I_{eq} + (1 - I_{eq}) \exp(-(t/T_0)^{\alpha})$. At much longer times, they decay exponentially. As an example for the applications of the equations derived in this section for



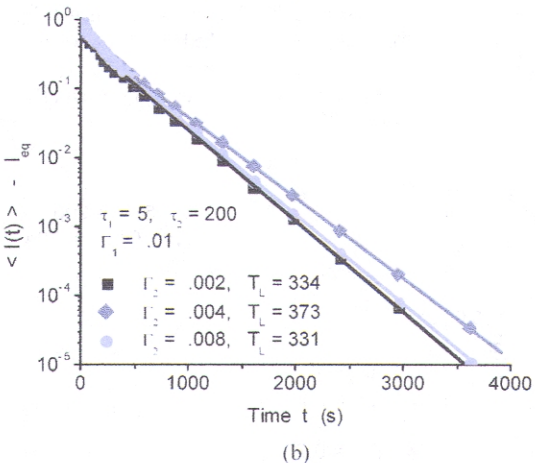


Fig. 11. (a) Semi-log plot of $\langle I(t) \rangle$ (dot curves) and the fitted (solid) curves using a stretched exponential $I_{eq} + (1 - I_{eq}) \exp(-(t/T_0)^{\alpha})$ with fitted values for α and T_{θ} . $\beta_{CD} = 1$ was used. 9(b) Semi-log plot of the normalized $\langle I(t) \rangle - I_{eq}$ showing a fitted tail of $\exp(-t/T_L)$, indicating the stretched exponential decay is only an approximation.

ensemble-averaged behavior, fluorescence intensity decay data of CdSe with a ZnS shell are compared with Eq. (22) as illustrated in Fig. 12. From the fits, we estimated some molecular-based kinetic and energetic parameters. As a comparison with the Debye case, which has normal diffusion in Fig. 11, anomalous diffusion is considered and the influence of β_{CD} is illustrated in Fig. 13. The fits to a stretched exponential for anomalous diffusion case are not as good as the normal diffusion case.

To obtain an analytic expression for $\langle I(t) \rangle$ or $\langle R(t) \rangle$ re-

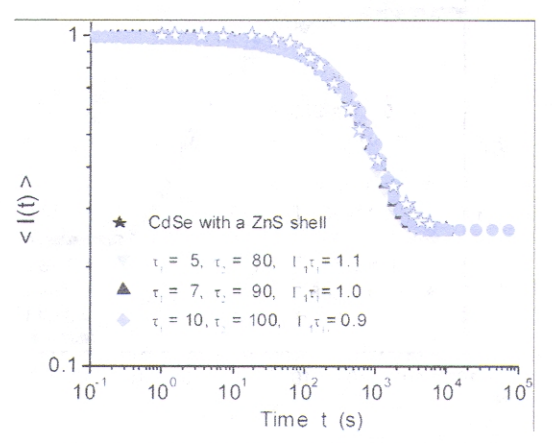


Fig. 12. Log-log plot of experimental $\langle I(t)\rangle$ (dot curves) and the fitted (solid) curves using Eq. (22). From $I_{eq} \sim 0.26$ at the long times, we estimated $\Delta G^0 \sim -33$ meV. Using $\xi_1 \sim 0.75$, $\tau_1 \sim 10$ s and $\tau_2 \sim 100$ s, we estimated $E_{A,I} \sim 45$ and $E_{A,2} \sim 78$ meV.³⁷

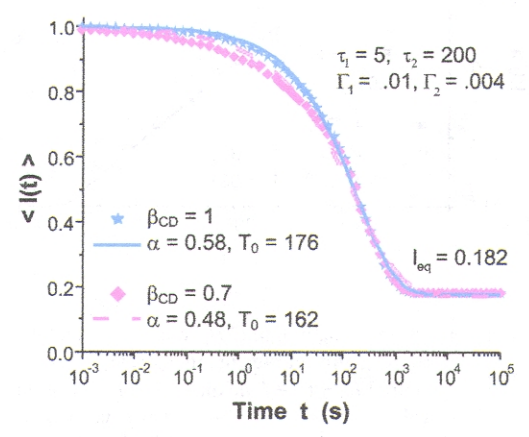


Fig. 13. Semi-log plot of $\langle I(t)\rangle$ vs. t for both normal and anomalous diffusion cases with a fit to a stretched exponential. As β_{CD} decreases the exponent α also decreases.

quires the inverse Laplace transform of Eqs. (21-23), and a closed form is unavailable. Instead, standard numerical inverse Laplace transform from IMSL was used to calculate $\langle I(t) \rangle$ and $\langle R(t) \rangle$. To obtain desired accuracy, we have included 25 terms in Taylor's series expansion of $\overline{g}_k(s)$ in either regime of a small and large s. The fitted values for τ_1 and τ_2 in Fig. 12 are not unique. We can obtain similar fits by varying τ_1 as much as 50% but keeping $\tau_1\Gamma_1$ fixed. Unique determination of Γ_1 requires measurements of the bending tail in $P_{on}(t)$ for a single QD under the same conditions of light intensity and temperature. Because diffusion is light-driven, an increase in light intensity shortens $\tau_{L,k}$ and increases Γ_k . From the analysis of the data of $\langle I(t) \rangle$ alone and the fitted $\tau_1\Gamma_1$, we are able to extract some useful parameters.

 $\langle \overline{I}(s) \rangle$ of Eq. (22) is related to the autocorrelation of fluorescence intensity of others by $\langle I(s) \rangle = \overline{C}_F(s)\gamma_2/(\gamma_1 + \gamma_2)$. As illustrated by experimental data of CdSe QDs by Messin et al., ¹⁸ with a very large time constant for a correlator, $C_F(t)/C_F(0)$ behaves as $\langle I(t) \rangle$ (or $\langle R(t) \rangle$ at short times). The fit to $1-C_F(t)/C_F(0)$, as shown in Fig. 14, shows a power law with $\beta_{CD}/2 \sim 0.48$, very close to the ideal value for normal diffusion ($\beta_{CD} = 1$). Unusual time dependence in $\langle I(t) \rangle$ and $\langle R(t) \rangle$ arises if $P_{onf}(t)$ and $P_{off}(t)$ follow different decaying laws. Such a situation has been extensively studied by Margolin and Barkai³⁵ using a phenomenological $P_k(t)$. It can be analyzed in this study by assigning a different β_{CD} for $\overline{g}_k(s)$ for the light and dark states. As an example, if $P_{off}(t)$ follows a power law but $P_{onf}(t)$ decays single expo-

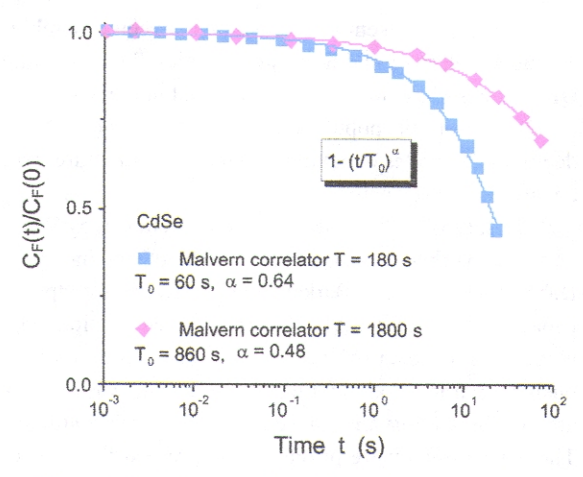


Fig. 14. Semi-log plot of $C_F(t)/C_F(0)$ for CdSe QDs fitted by power law $1 - (t/T_0)^{\alpha}$.

nentially as $\gamma_1 \exp(-\gamma_1 t)$, we obtain $C_F(t) \sim (t/t_{c,2})^{-\beta_{CD,2}/2} (\gamma_1 + \gamma_2)/\Gamma(1-\beta_{CD,2}/2)$ $\gamma_1\gamma_2$ $t_{c,2}$. Such a time dependence with $\beta_{CD,2} = 0.6$ was observed by Verberk et al. ²¹ in uncapped CdSe QDs. Both m for the exponent of P(t) and α for the stretched exponential fit to $\langle I(t) \rangle$ are influenced by the dielectric response, due to a distribution of diffusion correlation times. A correlation of m with dielectric properties was recently noted by Issac et al. ²⁴

For the anomalous diffusion case, the calculated $\langle I(t)\rangle$ is shown in Fig. 11 with a stretched exponential fit, and $\langle R(t)\rangle$ is illustrated in Fig. 15, showing $\langle R(t)\rangle\sim \exp(-(t/T_{s'})^{\beta_{CL'}/2})$ or $1-\langle R(t)\rangle\sim (t/T_s)^{\beta_{CL'}/2}$ at short times. $\langle R(t)\rangle$ approaches $\exp(-t/T_L)$ at longer times, where $T_L=(1+f_1+f_2)/(\gamma_1+\gamma_2)$ was derived from the asymptote of $\overline{g}_s(s)$

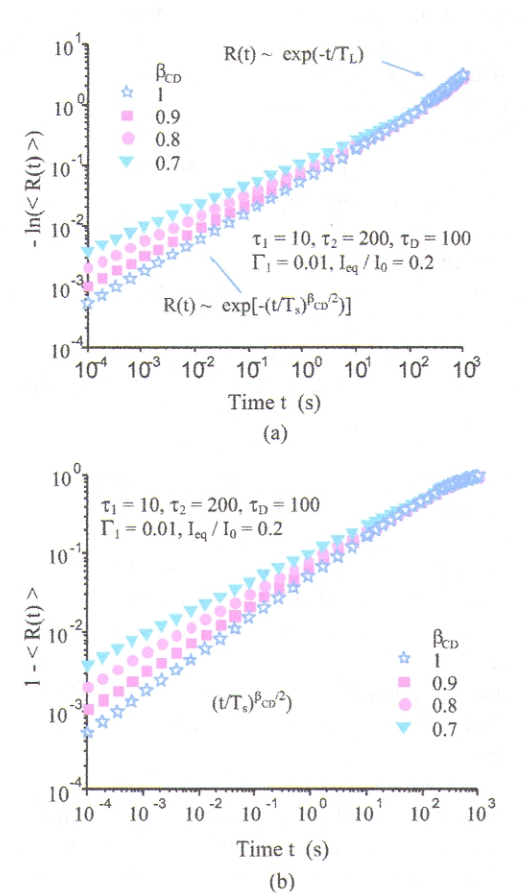


Fig. 15. (a) Log-log plot of $-\ln\langle R(t)\rangle$ vs. t. (b) log-log plot of $1-\langle R(t)\rangle$ vs. t. Both plots show a power law of $(t/T_{s'})^{\beta_{kD}/2}$ at a short time (t < 1 s). At longer times $(t >> 10^2 \text{ s})$, however, $\langle R(t)\rangle \sim \exp(-t/T_L)$.

at very small s. T_s can be derived from Eq. (22) as

$$(T_S)^{\beta_{CD}/2} = \frac{\Gamma(\beta_{CD}/2+1)}{(\gamma_1 + \gamma_2) \left((t_{c,1})^{1-\beta_{CD}/2} + (t_{c,2})^{1-\beta_{CD}/2} \right)}, (28)$$

which can be simplified for $\beta_{CD} = 1$ to

$$T_S = \frac{\pi^2}{8} \left(\frac{\sqrt{\tau_{L,1}} + \sqrt{\tau_{L,2}}}{\exp(-E_{A,1}/k_B T) + \exp(-E_{A,2}/k_B T)} \right)^2. \tag{29}$$

III. CONCLUSION

In conclusion, in this overview we have described recent developments in experiments and theories on fluorescence intermittency in quantum dots. Considerable improvement in understanding the underlying mechanism has been made possible by extensive studies by various groups. We have addressed five topics, including the issue about single particle vs. ensemble behavior, electronic states relevant to intermittency, photoinduced spectral diffusion, power-law intermittency, and ensemble-averaged fluorescence intensity decay. Using the diffusion-controlled electron transfer model for both normal and anomalous diffusion, we examined blinking behavior $P_k(t)$ for single QDs, ensemble-averaged fluorescence decay $\langle I(t) \rangle$, and the relationship between $\langle I(t) \rangle$ and relaxation function $\langle R(t) \rangle$ with $P_k(t)$, $\langle I(t) \rangle$, $\langle R(t) \rangle$ and $P_k(t)$ follow characteristically different decaying behavior during various time regimes. From the measurements of single-particle or ensemble behavior, one can in principle extract those molecular-based quantities. Applications were demonstrated with fittings to experimental data from single-QD studies and ensemble measurements.

Although in this report, we focused only on intermittency in quantum dots, the DCET model can be extended to similar power law behavior observed in single organic molecules. ^{29,30} The electronic structure for these systems are different from those of semiconductor materials; the fluorescence intermittency between a light state and a long-lived dark state is also believed to be controlled by 1-D diffusion in energy space. Extension of this DCET model to intermittency in enzyme activity using single molecule spectroscopy ⁵⁶ requires modification of the Marcus-type electron transfer reactions to Kramer's type of reactions in-

volving bistable potential. For a shallow bistable potential where its bottom is close to a sink, intermittency at short times is dictated by the diffusion near the bottom. One would expect similar power-law behavior as in QDs. More details await further investigation.

ACKNOWLEDGEMENT

The authors acknowledge the support of the National Science Foundation and the Office of Naval Research. J. T. is also thankful for the support from the James W. Glanville Foundation at the California Institute of Technology.

Received October 20, 2005.

REFERENCES

- Jacak, L.; Hawrylak, P.; Wojs, A. Quantum Dots; Springer: Berlin, 1997.
- Heiss, W. D., Ed. Quantum Dots: A Doorway to Nanoscale Physics; Springer: Berlin, 2005.
- 3. Botello, V., Ed. *Nanoparticles: Building Blocks for Nano-technology*; Kluwer Academic: New York, 2004.
- Parak, W. J.; Pellegrino, T.; Plank, C. Nanotech. 2005, 16, R9.
- Nirmal, M.; Dabbousi, B. O.; Bawendi, M. G.; Mackin, J. J.; Trautman, J. K.; Harris T. D.; Brus, L. E. *Nature* (London), 1996, 383, 802.
- 6. Krauss, T. D.; Brus, L. E. Phys. Rev. Lett. 1999, 83, 4840.
- Krauss, T. D.; O'Brien, S.; Brus, L. E. J. Phys. Chem. B 2001, 105, 1725.
- Nirmal, M.; Norris, D. J.; Kuno, M.; Bawendi, M. G.; Efros, A. L.; Rosen, M. Phys. Rev. Lett. 1995, 75, 3728.
- Empedocles, S. A.; Bawendi, M. G. J. Phys. Chem. B 1999, 103, 1826.
- Shimizu, K. T.; Neuhauser, R. G.; Leatherdale, C. A.;
 Empedocles, S. A.; Woo, W. K.; Bawendi, M. G. *Phys. Rev.* B 2001, 63, 205316.
- Shimizu, K. T.; Woo, W. K.; Fisher, B. R.; Eisler, H. J.;
 Bawendi, M. G. *Phys. Rev. Lett.* 2002, 89, 117401.
- 12. Chung, I.; Bawendi, M. G. Phys. Rev. B 2004, 70, 165304.
- Fisher, B. R.; Eisler, H-J.; Scott, N. E.; Bawendi, M. G. J. Phys. Chem. B 2004, 108, 143.
- Kuno, M.; Fromm, D. P.; Hamann, H. F.; Gallagher, A.;
 Nesbitt, D. J. J. Chem. Phys. 2000, 112, 3117.

- Kuno, M.; Fromm, D. P.; Hamann, H. F.; Gallagher, A.;
 Nesbitt, D. J. J. Chem. Phys. 2001, 115, 1028.
- Kuno, M.; Fromm, D. P.; Gallagher, A.; Nesbitt, D. J., Micic,
 O. I.; Nozik, J. J. Nano. Lett. 2001, 1, 557.
- Kuno, M.; Fromm, D. P.; Johnson, S. T.; Gallagher, A.;
 Nesbitt, D. J. Phys. Rev. B 2003 67, 125304.
- Messin, G.; Hermier, J. P.; Giacobino, E.; Desbiolles, P.;
 Dahan, M. Opt. Lett. 2001, 26, 1891.
- Michelet, X.; Pinaud, F.; Lacoste, T. D.; Dahan, M.; Bruchez, M. P.; Alivisatos, A. P.; Weiss, S. Sing. Mole. 2001, 2, 261.
- Brokmann, X.; Hermier, J. P.; Messin, G.; Desbiolles, P.;
 Bouchaud, J. P.; Dahan, M. Phys. Rev. Lett. 2003, 90, 120601.
- Verberk, R.; van Oijen, A. M.; Orrit, M. Phys. Rev. B 2002, 66, 233202.
- 22. Verberk, R.; Orrit, M. J. Chem. Phys. 2003, 119, 2214.
- Cichos, F.; Martin, J.; von Borczyskowski, C. *Phys. Rev. B* 2004, 70, 115314.
- Issac, A.; von Borczyskowski, C.; Cichos, F. *Phys. Rev. B* 2005, 71, 161302(R).
- Schlegel, G.; Bohnenberger, J.; Potapova, I.; Mews, A. Phys. Rev. Lett. 2002, 88, 137401.
- Pelton, M.; Grier, D. G..; Guyot-Sionnest, P. Appl. Phys. Lett. 2004, 85 819.
- Labeau, O.; Tamarat, P.; Lounis, B. Phys. Rev. Lett. 2003, 90, 257404.
- Biju, V.; Makita, Y.; Nagase, T.; Yamaoka, Y.; Yokoyama,
 H.; Baba, Y.; Ishikawa, M. J. Phys. Chem. B 2005, 109,
 14350.
- Hasse, M.; Hübner, C. G.; Reuther, E.; Herrmann, A.;
 Müllen, K.; Basche, T. J. Phys. Chem. B 2004, 108, 10445.
- Schuster, J.; Cichos, F.; von Borczyskowski, C. *Appl. Phys. Lett.* 2005, 87, 051915.
- 31. Efros, A. L.; Rosen, M. Phys. Rev. Lett. 1997, 78, 1110.
- 32. Wang, J.; Wolynes, P. J. Chem. Phys. 1999, 110, 4812.
- Boguna, M.; Berezhkovskii, A. M.; Weiss, G. H. *Physica A*, 2000, 282 475.
- Barkai, E.; Jung, Y.; Silbey, R. Annu. Rev. Phys. Chem. 2004, 55, 457; Jung, Y.; Barkai, E.; Silbey, R. J. Chem. Phys. 2002, 284, 181.
- 35. Margolin, G.; Barkai, E. J. Chem. Phys. 2004, 121, 1566.
- 36. Tang, J.; Marcus, R. A. J. Chem. Phys. 2005, 123, 054704.
- 37. Tang, J.; Marcus, R. A. Phys. Rev. Lett. 2005, 95, 107401.
- 38. Tang, J.; Marcus, R. A. J. Chem. Phys. 2005, 123, 204511.
- Frantsuzov, P. A.; Marcus, R. A. Phys. Rev. B, 2005, 72, 155321.
- Flomenbom, O.; Klafter, J.; Szabo, A. Biophy. J. 2005, 88, 3780
- 41. Osad'ko, I. S. Chem. Phys. 2005, 316, 99.

- 42. Zusman, D. Chem. Phys. 1980, 49, 295.
- 43. Sumi, H.; Marcus, R. A. J. Chem. Phys. 1986, 84, 4894.
- 44. Rips, I.; Jortner, J. J. Chem. Phys. 1987, 87, 6513.
- 45. Yan, J.; Sparpaglione, M.; Mukamel, S. J. Phys. Chem. 1988, 92, 842.
- 46. Seki, K.; Barzykin, A. V.; Tachiya, M. J. Chem. Phys. 1999, 110, 7639.
- 47. Bicout, D. J.; Szabo, A. J. Chem. Phys. 1998, 109, 2325.
- 48. Bouchaud, J. P.; Georges, A. Phys. Rep. 1990, 195, 127.
- 49. Hynes, J. T. J. Phys. Chem. 1986, 90, 3701.
- 50. Renger, T.; Marcus, R. A. J. Chem. Phys. 2002, 116, 9997.
- 51. Böttcherm, C. J. F.; Bordewijk, P. Theory of Electric Polar-

- ization; Vol. II Elsevier: Amsterdam, 1978.
- 52. Erdélyi, A.; Magnus, W.; Oberhettinger, F.; Tricomi, F. G. Higher Transcendental Functions; Vol. 1. Krieger: New York, 1981.
- 53. Rips, I.; Jortner, J. J. Chem. Phys. 1987, 87, 6513.
- 54. Bardou, F.; Bouchaud, J. P.; Aspect, A.; Cohen-Tannoudji, C. Lévy Statistics and Laser Cooling; Cambridge University Press: Cambridge, England, 2001.
- 55. Tang, J.; Marcus, R. A. (to be published).
- 56. Lu, H.; Xun, L.; Xie, X. S. Science 1998, 282, 1877; Vanden Bout, D. A.; Zhuang, X.; Xie, X. S., Ed., Acc. Chem. Res. 2005, 38, no. 7.